Superluminal geometrical resonances observed in $Bi_2Sr_2CaCu_2O_{8+x}$ intrinsic Josephson junctions

S. O. Katterwe,[1] A. Rydh,[1] H. Motzkau,[1] A. B. Kulakov,[2] and V. M. Krasnov[1,*]
[1]*Department of Physics, AlbaNova University Center, Stockholm University, SE-10691 Stockholm, Sweden*
[2]*Institute of Solid State Physics, Russian Academy of Sciences, 142432 Chernogolovka, Russia*
(Received 8 June 2010; revised manuscript received 29 June 2010; published 22 July 2010)

We study Fiske steps in small $Bi_2Sr_2CaCu_2O_{8+x}$ mesa structures, containing only a few stacked intrinsic Josephson junctions. Careful alignment of magnetic field prevents penetration of Abrikosov vortices and facilitates observation of a large variety of high-quality geometrical resonances, including superluminal with velocities larger than the slowest velocity of electromagnetic waves. A small number of junctions limits the number of resonant modes and allows accurate identification of modes and velocities. It is shown that superluminal geometrical resonances can be excited by subluminal fluxon motion and that flux flow itself becomes superluminal at high magnetic fields. We argue that observation of high-quality superluminal geometrical resonances is crucial for realization of the coherent flux-flow oscillator in the terahertz frequency range.

DOI: 10.1103/PhysRevB.82.024517 PACS number(s): 74.72.Gh, 74.78.Fk, 74.50.+r, 85.25.Cp

I. INTRODUCTION

Stacked Josephson junctions represent a macroscopic electromagnetic system which can be easily tuned from Lorentz invariant (uncoupled, single junctions[1,2]) to a noninvariant state by decreasing the layer thickness d below the magnetic screening length λ_S. The lack of Lorentz invariance is caused by the absence of local relation between electric and magnetic fields.[3] In thin-film stacks, $d \ll \lambda_S$, magnetic field is nonlocal and is created cooperatively by the whole stack, leading to inductive coupling of junctions.[4,5] The strongest coupling is achieved in atomic scale intrinsic Josephson junctions (IJJs), naturally formed in $Bi_2Sr_2CaCu_2O_{8+x}$ (Bi-2212) high-T_c superconductors. The lack of Lorentz invariance leads to a number of unusual electrodynamic properties, such as splitting of the dispersion relation of electromagnetic waves,[6] and a possibility of superluminal (faster than the slowest electromagnetic wave velocity) motion of Josephson vortices (fluxons), accompanied by Cherenkov-type radiation.[3,7–9] The coupling facilitates phase locking of junctions, which may lead to coherent amplification of the emission power[5,10,11] $\propto N^2$, where N is the number of junctions. IJJs allow easy integration of many strongly coupled stacked junctions. Furthermore, the large energy gap in Bi-2212 (Ref. 12) facilitates operation in the important terahertz (THz) frequency range. Therefore, IJJs are intensively studied as possible candidates for realization of a coherent THz oscillator.[9,13–27] A variety of different emission mechanisms from IJJs are considered, including emission via resonant excitation of Josephson plasma waves at zero magnetic field,[13,14,22–25,27] direct emission upon relaxation of nonequilibrium quasiparticles (QPs),[20] Cherenkov radiation from superluminal fluxons,[3,7–9] and flux-flow emission generated upon collision and annihilation of fluxons with the edge of the stack at large in-plane magnetic fields.[15–19,26] The latter mechanism is relevant for the present work.

The flux-flow oscillator (FFO) is based on regular, unidirectional motion of fluxons in Josephson junctions.[28] To facilitate coherent emission from a stacked FFO, fluxons in the stack must be arranged in a rectangular (in-phase) lattice. It can be stabilized by geometrical confinement in small Bi-2212 mesa structures[29] at high magnetic fields $B \sim \Phi_0/s\lambda_J \simeq 2$ T, where Φ_0 is the flux quantum, $s=1.55$ nm is the interlayer spacing, and λ_J is the Josephson penetration depth of IJJs. At lower fields flux flow is metastable or chaotic.[8,30] Yet, the rectangular lattice is insufficient for achieving high emission power from the FFO. Since the power is proportional to the square of the electric field amplitude E_{ac}, a large E_{ac} should also be established.[26] In a single junction FFO (Ref. 28) this is achieved via Lorentz contraction of fluxons[1,2] $\lambda_J \propto \sqrt{1-(u_{FF}/c_0)^2}$, where u_{FF} is the fluxon velocity and c_0 is the (Swihart) velocity of light in a single junction. Consequently, the electric field at the fluxon origin $E_{ac}(0) \propto \partial\varphi/\partial t = u_{FF}\partial\varphi/\partial x \propto u_{FF}/\sqrt{1-(u_{FF}/c_0)^2}$, where φ is the Josephson phase difference, increases dramatically at the velocity-matching condition $u_{FF} \to c_0$.[1] However, such a mechanism is not available in stacked junctions due to the absence of Lorentz invariance in the system.[3] Numerical simulations have shown that a partial Lorentz contraction of the fluxon at $u_{FF} \to c_N$ occurs only in double stacked junctions.[31] For $N>3$, Lorentz contraction of the fluxon is absent[3] and fluxon's electric field increases only gradually, $E_{ac}(0) \propto u_{FF}$, at the velocity-matching condition $u_{FF} \to c_N$. As emphasized in Ref. 26, under such circumstances powerful emission is only possible in the presence of high-quality $Q \gg 1$ geometrical (Fiske) resonances, which would enhance the oscillating electric field in the stack $E_{ac} \propto Q$. Thus, observation of high-speed and high-quality geometrical resonances is a prerequisite for realization of the high-power coherent FFO.

For artificial low-T_c stacked Josephson junctions both velocity splitting[4,5] and coherent amplification of radiation[11] were observed experimentally. However, for IJJs only the slowest out-of-phase Fiske steps have been unambiguously detected.[32–34] Observation of superluminal resonances in IJJs may be obscured by several factors: for stacks with a large number of IJJs, $N \sim 100$, the velocity splitting may be too dense to be identified and the exact number of junctions in the flux-flow state difficult to estimate. The necessity to operate in large magnetic fields may also lead to intrusion of Abrikosov vortices that distort fluxon order and dampen resonances.[29,35] Coherently emitting resonant modes can be

dampen by radiative losses[26] and, as discussed below, high-frequency resonances are very sensitive to a spread in junction resistances.

In this work we study Fiske steps in small Bi-2212 mesa structures containing only few IJJs. Careful alignment of magnetic field parallel to CuO planes obviates intrusion of Abrikosov vortices and leads to observation of a large variety of high-quality geometrical resonances with different velocities. Small N limits the number of resonant modes and simplifies their identification. We demonstrate both experimentally and numerically that superluminal geometrical resonances are excited by subluminal flux flow. Simultaneously we observe that flux flow itself becomes superluminal at high magnetic fields. Finally we observe an asymmetry between even and odd resonance modes, which can be taken as indirect evidence for considerable flux-flow emission from the stack.[26]

II. GENERAL RELATIONS

Inductive coupling of N stacked Josephson junctions leads to splitting of the dispersion relation of electromagnetic waves into N branches with characteristic velocities[6]

$$\frac{c_n}{c_0} = \left[1 - 2S\cos\frac{n\pi}{N+1}\right]^{-1/2} \quad (n = 1,2,\ldots,N). \tag{1}$$

Here $S \simeq 0.5/\cosh(d/\lambda_S)$ is the coupling constant. Since there has been some confusion about values of extremal velocities in IJJs, we want to provide explicit expressions for c_N and c_1 in terms of material parameters. Following the formalism of Refs. 3 and 8 we obtain

$$c_N \simeq \frac{c}{2}\sqrt{\frac{ts}{\varepsilon_r\lambda_{ab}^2}}\left[1 + \frac{1}{8}\left(\frac{s^2}{\lambda_{ab}^2} + \frac{\pi^2}{(N+1)^2}\right)\right], \tag{2}$$

$$c_1 \simeq c\sqrt{\frac{ts}{\varepsilon_r\lambda_{ab}^2}}\left[\frac{s^2}{\lambda_{ab}^2} + \frac{\pi^2}{(N+1)^2}\right]^{-1/2}. \tag{3}$$

The accuracy of expansion is $\mathcal{O}\{(s/\lambda_{ab})^4 + [\pi/(N+1)]^4\}$. Here $c = 3\times 10^8$ m/s is the velocity of light in vacuum, $\lambda_{ab} = \lambda_S[s/d]^{1/2}$ is the effective London penetration depth, and $t = s - d$ and ε_r are the thickness and the relative dielectric permittivity of the junction barrier, respectively. The ratio $t/\varepsilon_r \simeq 0.1$ nm, corresponding to reasonable values of the double-CuO layer thickness $d \simeq 0.6$ nm and $\varepsilon_r \simeq 10$, can be deduced from previous studies of Fiske steps in IJJs.[32–34] The first expansion term $(s/\lambda_{ab})^2 \simeq 6\times 10^{-5}$ is small and can be neglected in Eq. (2) for all N and in Eq. (3) for $N \ll \pi\lambda_{ab}/s \simeq 400$. This leads to further simplification,

$$c_N \simeq \frac{c}{2}\sqrt{\frac{ts}{\varepsilon_r\lambda_{ab}^2}} = \frac{c_0}{\sqrt{2}}, \tag{4}$$

$$c_1 \simeq c\sqrt{\frac{ts}{\varepsilon_r\lambda_{ab}^2}}\frac{N+1}{\pi} \simeq \frac{2(N+1)}{\pi}c_N. \tag{5}$$

The accuracy of this expansion is $\mathcal{O}[(s/\lambda_{ab})^2 + (N+1)^{-2}]$.

The above expressions allow straightforward estimation of extremal velocities in IJJs. The slowest velocity $c_N \simeq (3.0 \pm 0.6)\times 10^5$ m/s is almost independent of N. Here, the central value corresponds to optimal doping with $\lambda_{ab} \simeq 200$ nm and plus/minus corrections to overdoped/underdoped Bi-2212 with smaller/larger λ_{ab}, correspondingly. The fastest velocity c_1, by contrast, is not universal and increases almost linearly with N. For typical IJJ numbers used in previous studies, $c_1(N=30) \simeq 6\times 10^6$ m/s and $c_1(N=100) \simeq 1.9\times 10^7$ m/s. Experimentally reported maximum flux-flow velocities are on the order of c_N (Refs. 7, 15, 30, and 32–37) and substantially smaller than c_1 for the corresponding number of IJJs. According to numerical simulations[16,17] the rectangular lattice is unconditionally stable only at fast superluminal velocities $c_2 < u_{FF} < c_1$, which have not been reached in experiments so far. Although the rectangular lattice can be stabilized in the static case by geometrical confinement in small mesas,[29] it tends to reconstruct into the triangular lattice at slow flux-flow velocities $u_{FF} < c_N$.[16–19] Therefore, the stability of the rectangular fluxon lattice is remaining a critical issue for the realization of a coherent FFO.

At high in-plane magnetic fields $B > \Phi_0/s\lambda_J$ fluxons form a regular lattice in the stack. This brings about phononlike collective excitations, which can be characterized by two wave numbers[6] $k_m = m\pi/L$ $(m = 1,2,3,\ldots)$ in plane and $q_n = n\pi/Ns$ $(n = 1,2,\ldots,N)$ in the c-axis direction. Here L is the in-plane length of the stack. Unlike Josephson plasma waves, fluxon phonons have a linear dispersion relation at low frequencies.[38] Fluxon phonons with mode (m,n) propagate with the in-plane velocity c_n of Eq. (1). The slowest velocity c_N $(q_N = \pi/s)$ corresponds to out-of-phase oscillation in neighbor junctions, the fastest c_1 $(q_1 = \pi/Ns)$ to in-phase oscillation of all junctions. Fluxon phonons can be excited in the flux-flow state. Geometric resonances occur when the ac-Josephson frequency $\omega_J = 2\pi V_{FF}/\Phi_0$ coincides with the frequency $\omega_{m,n}$ of one of the modes (m,n). Here

$$V_{FF} = u_{FF}Bs \tag{6}$$

is the dc flux-flow voltage per junction. The resonances can be seen as a series of Fiske steps at voltages (per junction)

$$V_{m,n} = \frac{\Phi_0}{2L}mc_n \quad (m = 1,2,3,\ldots,\ n = 1,2,\ldots,N). \tag{7}$$

The (almost) linear dispersion relation of fluxon phonons makes Fiske steps with a given n (almost) equidistant in voltage both for single[39,40] and stacked[5] junctions.

From comparison of Eqs. (6) and (7) it follows that modes with velocity c_n can be excited at $u_{FF} < c_n$ provided that

$$\frac{u_{FF}}{c_n} \geq \frac{\Phi_0}{2\Phi}, \tag{8}$$

where $\Phi = BLs$ is the flux per junction. The strongest coupling between resonant modes and flux flow occurs when fluxons propagate with the same velocity as fluxon phonons, $u_{FF} = c_n$ (the velocity-matching condition) and the in-plane wavelength of the standing wave is equal to the separation between fluxons. This happens when

TABLE I. Summary of studied mesas. N is the number of junctions in the mesa. L and w are the nominal in-plane mesa sizes in directions perpendicular and parallel to the field, respectively. $L_{\rm eff}=\Phi_0/B_0 s$ is the effective length calculated from the observed flux-quantization field B_0. J_c is the critical current density at $B=0$. $V_{1,N}$ is the voltage of the lowest out-of-phase Fiske step and c_N is the corresponding slowest velocity of electromagnetic waves. The pure and lead-doped Bi-2212 crystals are slightly underdoped and overdoped, respectively.

Mesa	Crystal	N	T_c (K)	L (μm)	w (μm)	$L_{\rm eff}$ (μm)	B_0 (T)	J_c (kA/cm^2)	λ_J (μm)	$V_{1,N}$ (mV)	c_N (10^5 m/s)
1	Bi-2212	8	82	2.7	1.4	2.43	0.55	1.1	0.69	0.135 ± 0.005	3.17 ± 0.15
2	Bi-2212	11	89	1.0	1.0	1.60	0.82	1.1	0.67	0.185 ± 0.010	2.88 ± 0.20
3	Bi(Pb)-2212	≈15	87	0.6	1.1	0.53	2.54	11.5	0.20	0.64 ± 0.04	3.3 ± 0.2
4	Bi(Pb)-2212	≈56	87	1.2	2.0	1.13	1.21	7.3	0.26	0.38 ± 0.02	3.9 ± 0.2

$$m^* = 2\Phi/\Phi_0. \quad (9)$$

Therefore, the most prominent Fiske steps should correspond to the velocity-matching modes (m^*,n), even in the absence of Lorentz contraction of the fluxon. Steps with odd and even m should modulate in antiphase with each other[39] and have maximum amplitudes at integer and half integer Φ/Φ_0, respectively.[32,33] This additional selection rule can make $m=m^*-1$ resonances stronger than $m=m^*$.

III. EXPERIMENTAL

Two batches of Bi-2212 single crystals were used in this work: pure Bi-2212 and lead-doped $Bi_{2-y}Pb_ySr_2CaCu_2O_{8+x}$ [Bi(Pb)-2212] single crystals. The most noticeable difference between those crystals is in the c-axis critical current density J_c, which is larger by an order of magnitude for Bi(Pb)-2212, see Table I. Comparing with the doping dependence of J_c in IJJs (Ref. 41) we conclude that Bi-2212 crystals are slightly underdoped and Bi(Pb)-2212 slightly overdoped.

Small mesa structures were fabricated at the surface of freshly cleaved crystals by means of photolithography, Ar milling, and focused ion-beam trimming. Details of mesa fabrication are described elsewhere.[42] Several mesas with different dimensions were studied, all of them showed similar behavior. The number of junctions in the mesas N was obtained by counting QP branches at $B=0$, see Fig. 1. Mesa properties are summarized in Table I.

Samples were mounted on a rotatable sample holder and carefully aligned to have $B\|ab$. Accurate alignment is critical for the resonant phenomena reported below. To avoid field lock-in hysteresis, the alignment was done by minimizing the high-field and high-bias QP resistance.[29] After alignment all mesas exhibited clear Fraunhofer-type modulation of the critical current[29] $I_c(B)$ with the flux-quantization field B_0, see Table I. This allows estimation of the actual junction length, perpendicular to the field, $L_{\rm eff}=\Phi_0/B_0 s$. It is usually only slightly different from the nominal mesa size L obtained from the surface inspection by scanning electron microscopy. Fiske steps were observed in all studied mesas after proper alignment. Measured values of the lowest Fiske step $V_{1,N}$ and the corresponding lowest velocities c_N are given in Table I. Step voltages are inversely proportional to mesa lengths, as expected from Eq. (7).

All measurements were performed at $T=1.6$ K. I-V characteristics are presented as digital oscillograms (intensity plots) and were obtained by measuring voltage and current over several current sweeps. The contact resistance originating from the deteriorated topmost IJJ (Ref. 12) was numerically subtracted from all I-V characteristics.[29] Subtraction works very well in the whole flux-flow region with the accuracy ~10 μV (cf. supercurrent branches in the figures below). It simplifies data analysis and does not affect results in any way.

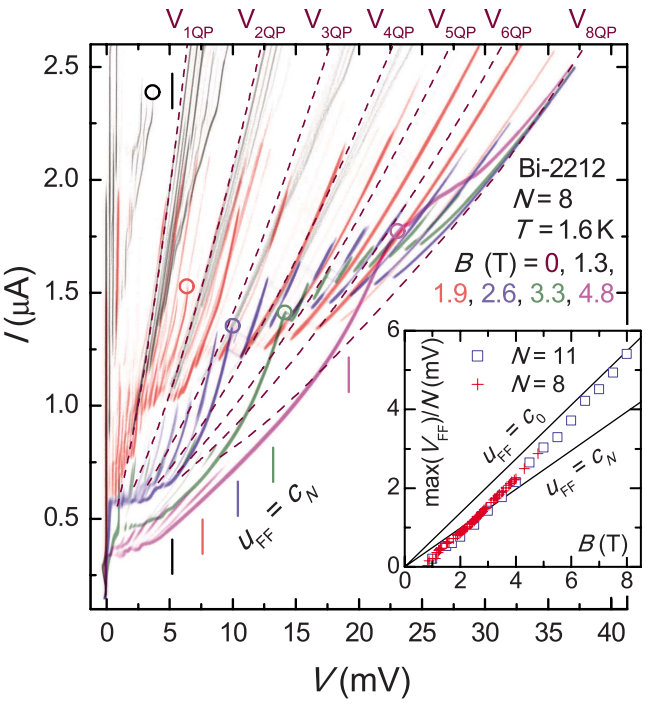

FIG. 1. (Color online) I-V characteristics of mesa 1 at different magnetic fields. Dashed lines represent quasiparticle branches at $B=0$. Development of flux-flow branches with increasing field is clearly seen. Circles mark maximum flux-flow voltages. Short lines indicate the velocity-matching condition $u_{\rm FF}=c_8$. Inset: the maximum flux-flow voltage per junction vs B for mesa 1 ($N=8$) and mesa 2 ($N=11$). Lines correspond to flux-flow velocities equal to c_N and c_0, respectively. It is seen that the experimentally observed flux-flow velocity becomes superluminal, $u_{\rm FF}>c_N$, at $B>2.6$ T and approaches the Swihart velocity c_0 at high fields.

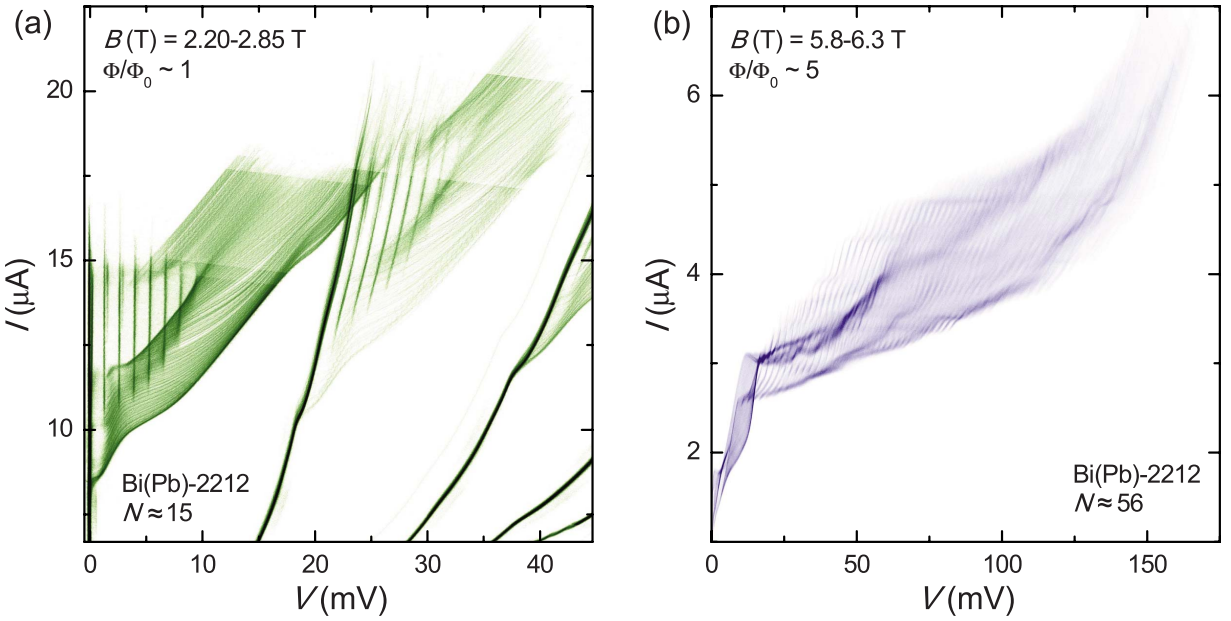

FIG. 2. (Color online) *I-V* oscillograms for continuous field sweeps around integer flux quanta per junction for Bi(Pb)-2212 mesas (a) 3 and (b) 4. At low fields in (a) both the continuously varying viscous flux-flow state and sharp, vertical, equidistant Fiske steps are simultaneously observed. At higher fields in (b) the whole flux-flow oscillogram is stratified into dense grids of resonances. This clearly demonstrates that the flux-flow *I-V* characteristics in this case are not changing continuously with field but switch between a variety of distinct resonant states.

IV. RESULTS AND DISCUSSION

A. Flux flow and Fiske steps

Figure 1 shows *I-V* oscillograms of mesa 1 at different magnetic fields from 0 to 4.8 T. At $I > I_c$, fluxons start to move and soon all eight IJJs are in the flux-flow state with a total voltage $V_{8FF} \sim 8V_{FF}$, where V_{FF} is the flux-flow voltage per junction. When one of the junctions switches to the QP state, seven junctions remain in the flux-flow state and the first combined QP-FF branch appears at $V = V_{1QP} + V_{7FF}$. When the next IJJ switches to the QP state the second combined QP-FF branch appears at $V = V_{2QP} + V_{6FF}$, then at $V = V_{3QP} + V_{5FF}$, and so on.[43] For identical junctions $V_{iQP} = iV_{QP}$ and $V_{iFF} \approx iV_{FF}$. The separation between such combined QP-FF branches is $V_{QP} - V_{FF}$ and is decreasing with increasing field to finally disappear at $B \sim 5.8$ T (not shown). This is consistent with previous observations.[15] What is different is the presence of remarkably strong Fiske steps at every QP-FF branch.

Figure 2 shows oscillograms collected during continuous field sweeps for Bi(Pb)-2212 mesas 3 and 4. It is clearly seen that the flux-flow characteristics are not continuous but are composed of a sequence of distinct Fiske steps, much like the case of strongly underdamped low-T_c junctions.[28] We emphasize that such high-quality geometrical resonances are observed only after careful alignment of the sample. Even a small misalignment of $\sim 0.1°$ leads to an avalanchelike entrance of Abrikosov vortices at high fields, which completely suppresses both these spectacular Fiske steps and the Fraunhofer modulation of the critical current.[29]

Unambiguous identification of the resonance modes (m,n) requires first of all discrimination between individual (not phase-locked) and collective (phase-locked) Fiske steps. This is nontrivial because, for instance, the voltage $1V_{m,1}$ of an individual in-phase step is close to the voltage $NV_{m,N}$ of a collective out-of-phase step, see Eqs. (4) and (5). Besides, not all junctions may participate in the collective resonance. For mesas with large $N > 10$ different resonant modes (m,n) form a very dense, almost continuous, Fiske step sequence. Therefore, bare analysis of voltage spacings is insufficient. To simplify discrimination between modes with different velocities, mesas with small N should be analyzed. Below we mainly focus on mesa 1 with the smallest number of IJJs $N = 8$.

Figure 3 shows *I-V* oscillograms of mesa 1 in narrow field ranges corresponding to half-integer and integer number of flux quanta Φ/Φ_0 per IJJ. To check whether the observed Fiske steps are individual or collective, in the inset of Fig. 3(a) we compare steps at the first V_{8FF} flux-flow branch and the second V_{7FF} (with one junction in the QP state). To obtain V_{7FF}, the first QP voltage $V_{1QP}(B=0)$ is subtracted from the $V_{1QP} + V_{7FF}$ branch. Collective steps should decrease in proportion to the number of junctions, e.g., 7/8 times. Individual steps, on the other hand, should maintain the same voltage at both flux-flow branches. This is the case at half integer Φ/Φ_0 in Figs. 3(a) and 3(b). The dominant step at integer $\Phi/\Phi_0 \simeq 3$, see Fig. 3(c), however, occurs at $8V_{1,8}$ at the V_{8FF} branch and at $7V_{1,8}$ at the next V_{7FF} branch, and is thus collective. Discrimination between individual and collective steps allows accurate identification of resonant modes (m,n).

The smallest step sequence $\simeq 0.135$ mV is observed at integer Φ/Φ_0, see Fig. 3(c). It corresponds to the expected value $V_{1,8}$ for the lowest odd $m=1$ out-of-phase $n=8$ individual Fiske step. The corresponding slowest velocity $c_8 \simeq 3.17 \times 10^5$ m/s is consistent with the estimation from Sec.

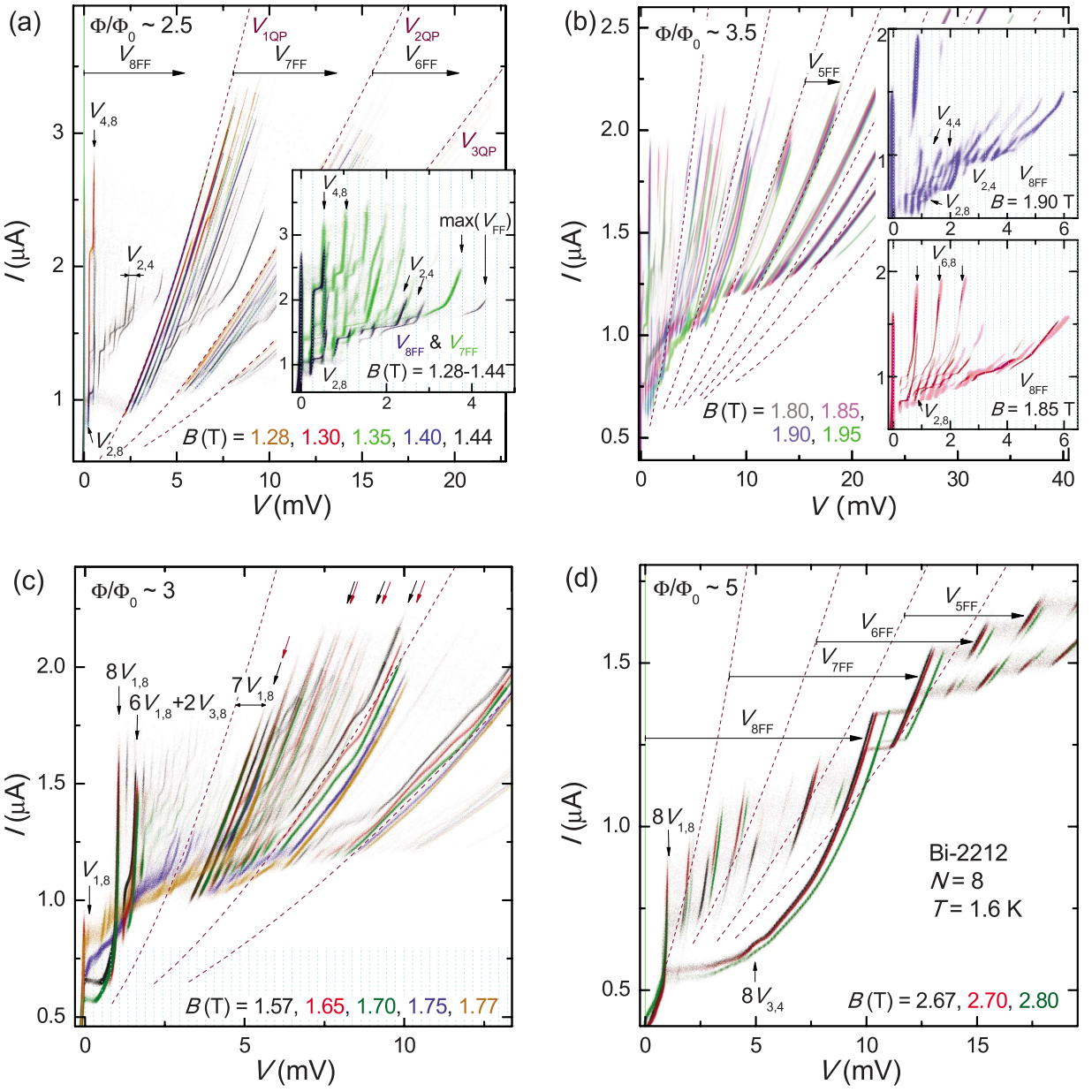

FIG. 3. (Color online) I-V oscillograms of mesa 1 (at constant B) in narrow field ranges near [(a) and (b)] half integer and [(c) and (d)] integer Φ/Φ_0. A large variety of high-quality Fiske steps are seen. Also shown are the QP branches at $B=0$ (dashed lines). The grid spacing is $V_{2,8}=0.27$ mV. The inset in (a) shows Fiske steps at the flux-flow branches with zero (V_{8FF}) and one (V_{7FF}) IJJ in the QP state, respectively. Voltage separation between steps is clearly independent of the number of junctions, showing that the Fiske steps here are from individual IJJs. The insets of panel (b) show the low-bias region at $B=1.85$ and 1.90 T. Several individual Fiske steps are marked. At integer Φ/Φ_0 in (c), by contrast, the prominent collective step $NV_{1,8}$ is seen, which scales with the number of junctions for V_{8FF} and V_{7FF}. Two collective steps are also indicated in (d). Thus, IJJs behave more individually or collectively at half integer or integer Φ/Φ_0, respectively.

II. Simultaneously, a strong collective Fiske step at $V=8V_{1,8}$ is observed, as marked in Figs. 3(c) and 3(d). It corresponds to the phase-locked state of the whole mesa at the same (1,8) resonance. Steps with separation $2V_{1,8}$ are seen above the collective step in Fig. 3(c). They are due to switching between nearest odd $m=1$ and $m=3$ out-of-phase $n=8$ resonances in individual IJJs, consistent with numerical simulations below.

At half integer Φ/Φ_0 the smallest step sequence corresponds to the lowest even $m=2$ individual Fiske step $V_{2,8}$ $\simeq 0.27$ mV, marked in Fig. 3(a) and insets of Fig. 3(b). The most prominent Fiske steps at half integer Φ/Φ_0 correspond to individual even $m=4$ and $m=6$ out-of-phase resonances in Figs. 3(a) and 3(b), respectively, which are close to the velocity-matching condition of Eq. (9).

While the Fiske step patterns vary significantly with magnetic field, they have certain common features for integer (more collective behavior, odd-m modes) and half integer (more individual behavior, even-m modes) Φ/Φ_0. The step amplitudes oscillate strongly with B, with odd and even m in

TABLE II. Calculated characteristic velocities c_n for mesa 1, using $s=1.55$ nm, $\lambda_{ab}=200$ nm, and $t/\varepsilon_r=0.112$ nm and Eq. (1). Also given are the ratios c_n/c_8 and calculated Fiske step voltages $V_{1,n}=B_0 s c_n/2$, where $B_0=0.55$ T is the flux-quantization field.

n	1	2	3	4	5	6	7	8
c_n (10^5 m/s)	17.97	9.13	6.24	4.86	4.08	3.60	3.32	3.17
c_n/c_8	5.67	2.88	1.97	1.53	1.29	1.14	1.05	1.00
$V_{1,n}$ (mV)	0.765	0.389	0.266	0.207	0.174	0.153	0.141	0.135

antiphase with each other, as expected. A complete overview of the modulation can be found in the supplementary material.[44]

B. Superluminal resonances

So far, we discussed out-of-phase Fiske steps with voltages equal to multiple integers of $V_{1,8}$. Such steps, both individual[45] and collective,[32,33] with similar velocities $c_N=2.5-3.5\times10^5$ m/s were observed previously, although with smaller relative amplitudes. However, in our case the full set of observed Fiske steps cannot be described solely by multiple integers of $V_{1,8}$. We can distinguish step sequences with different voltage spacings, which must correspond to resonances with higher velocities $c_n>c_8$, listed in Table II.

In the flux-flow region V_{7FF} of Fig. 3(c), where one IJJ has switched to the QP state, two sequences of steps with slightly different voltage spacings are seen at 1.57 T (black) and 1.65 T (red curve). Both step sequences start from the same $7V_{1,8}$ level, corresponding to the collective (1,8) geometrical resonance in the remaining seven IJJs. The lowest (black) step sequence has a step separation of $4V_{1,8}$ and is due to sequential switching of junctions from the lowest odd resonance (1,8) to the odd resonance (5,8) closest to the velocity-matching condition at the same speed. The whole step sequence is then described by $V_i=(7-i)V_{1,8}+iV_{5,8}$, where $i=0,1,\ldots,7$ is the number of junctions in the (5,8) state and the separation between steps is $V_{5,8}-V_{1,8}=4V_{1,8}$. The higher (red) step sequence also starts from the same $7V_{1,8}$ level but the splitting between the two step sequences becomes progressively larger with increasing step number, as indicated by black and red arrows for step numbers 3 and 5 in Fig. 3(c). This step sequence is described by a similar expression $V_i=(7-i)V_{1,8}+iV_{m,n}$ $(i=0,1,\ldots,7)$. The corresponding eight (red) Fiske steps can be distinguished in Fig. 3(c). The involved resonance $V_{m,n}=1.05V_{5,8}$ is very close to $V_{5,7}$, which represents the first superluminal resonance $n=7$, see Table II.

Individual step sequences

$$V_i=(N-i)V_{1,8}+iV_{m,n} \quad (i=0,1,\ldots,N)$$

are observed at all integer Φ/Φ_0. At $\Phi/\Phi_0\simeq5$ in Fig. 3(d), for example, nine steps can be distinguished on the $8V_{FF}$ branch. At a first glance they may look similar to previously seen subbranching due to onset of uncorrelated viscous flux flow in individual IJJs.[15] However, steps discussed here are resonant. In contrast to viscous flux-flow branches, which change monotonously with field, see Fig. 2(a), these steps are periodically modulated in magnetic field[44] and the step voltage is not changing continuously, but goes through discrete, although dense, set of values, see Fig. 2(b). This leads to the small splitting of steps in Fig. 3(c). Splitting of steps number 2–4 is also seen in Fig. 3(d). At certain conditions different step sequences can be observed at the same B, leading to a fine splitting as shown in the bottom inset of Fig. 3(b). The appearance of different step sequences is due to discrete, rather than continuous, change in the flux-flow voltage with B.

At $\Phi/\Phi_0\sim2.5$, see Fig. 3(a), an individual step sequence with a voltage spacing of 0.42 mV is observed both in the flux-flow regions V_{8FF} and V_{7FF}. The ratio of this voltage spacing to $V_{2,8}$ is 1.55, which is close to the ratio expected for $c_4/c_8=1.53$, see Table II. We, therefore, identify this voltage spacing with $V_{2,4}$. At the next half integer $\Phi/\Phi_0\sim3.5$ we observe two even-m resonances for the same $n=4$ mode, $V_{2,4}$ and $V_{4,4}$, as indicated in the top inset of Fig. 3(b). In Fig. 3(d), an additional collective step is seen at $V\simeq5$ mV when the current is decreased from high bias. It may correspond to a phase-locked $8V_{3,4}$ Fiske step, or possibly $8V_{4,6}$.

C. Fiske step modulation

The main panel in Fig. 4(a) shows Fraunhofer-type modulation of the critical current for mesa 1. Dashed vertical lines indicate the magnetic fields at integer Φ/Φ_0. Dominant and subdominant maxima of $I_c(\Phi)$ at half integer and integer Φ/Φ_0 correspond to rectangular and triangular fluxon lattices, respectively.[29] Fiske steps also modulate strongly with magnetic field, as shown in the lower inset of Fig. 4(a) for several prominent steps. It is expected that steps with even m modulate in phase with $I_c(\Phi)$, i.e., have maxima at half integer Φ/Φ_0. Steps with odd m modulate out of phase with $I_c(\Phi)$ and have maxima at integer Φ/Φ_0. Voltages of the chosen prominent Fiske steps are shown in the upper inset. Variation in the voltage demonstrates that switching between modes with different m and n occurs with variation in field.

Figure 4(b) summarizes our main experimental results. It shows a probability histogram for all observed step voltage spacings in the field interval up to $B=4$ T. The step at $V_{2,8}\simeq0.27$ mV has the highest number of counts. However, vertical lines in the upper part of the figure indicate that all experimentally observed steps cannot be described solely by $(m,8)$ resonances. To explain the rich variety of steps, geometrical resonances with different velocities have to be present. Exact identification of all steps is rather complicated because velocity splitting creates rather dense and often overlapping voltage sequences even for $N=8$. Expected volt-

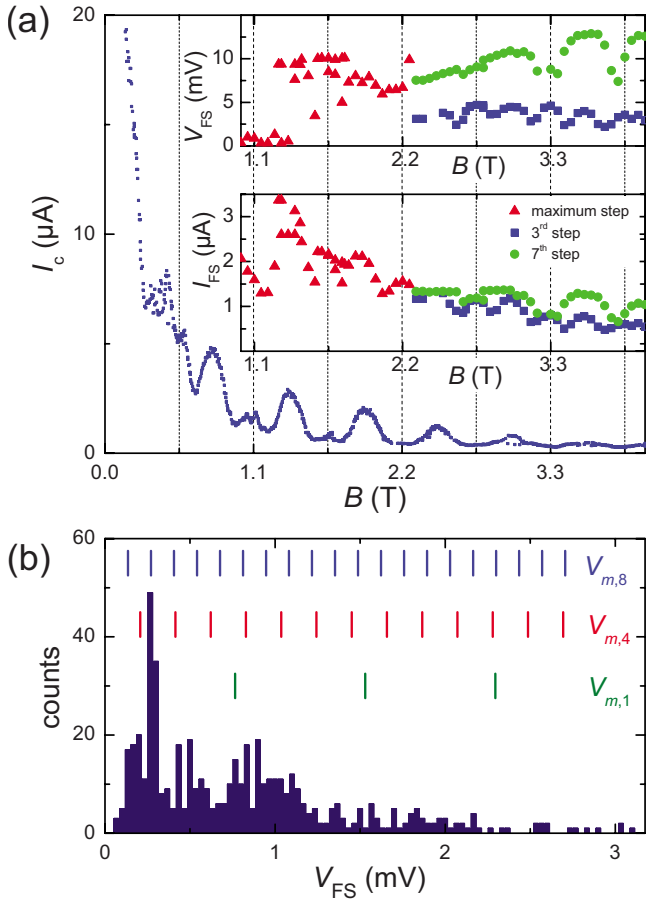

FIG. 4. (Color online) (a) $I_c(B)$ pattern for mesa 1. Grid lines corresponds to integer Φ/Φ_0. The lower inset shows modulation of amplitudes of some prominent Fiske steps. Triangles represent the Fiske steps with the highest amplitude at fields from 1 to 2.25 T. Squares and circles represent the third, respectively, seventh step in individual Fiske step sequences at high bias at $B>2.3$ T [as in Fig. 3(d) at 0.5 μA$<I<$1.5 μA]. Voltages of the same steps are shown in the upper inset. (b) Probability histogram for observation of different steps separations in the field interval from 0 to 4 T. Top vertical lines indicate out-of-phase Fiske steps, which are multiple integers of $V_{1,8}$. Apparently all observed steps cannot be described solely by out-of-phase resonances. Expected voltages for $n=4$ and $n=1$ superluminal steps are also indicated.

age positions for individual superluminal $n=4$ and $n=1$ Fiske steps are indicated in Fig. 4(b).

D. Maximum flux-flow velocity

Since we have confidently identified the slowest velocity of light $c_8=3.17\times10^5$ m/s, it is instructive to compare it with the maximum flux-flow velocity. In Fig. 1 voltages at the velocity-matching condition $u_{FF}=c_8$ and maximum flux-flow voltages are marked by short lines and circles, respectively. It is seen that the maximum flux-flow velocity is less, equal, and larger than c_8 for fields less, equal, and larger than 2.6 T. Interestingly, nothing special happens with the flux-flow branch when it becomes superluminal, $u_{FF}>c_N$. This is consistent with numerical simulations[3] and is due to the absence of Lorentz contraction of fluxons in strongly coupled, stacked Josephson junctions. The inset in Fig. 1 shows measured maximum flux-flow voltages per junction for mesas 1 and 2. The lines represent flux-flow voltages with velocities $c_N=3.17\times10^5$ m/s and $c_0=4.42\times10^5$ m/s. Gradual increase in the maximum flux-flow velocity with field is clearly seen and is consistent with previous reports.[7,30,32,34,37] The maximum u_{FF} is approaching c_0 at high fields. A similar limiting velocity was obtained by numerical simulations for the case when fluxon stability is limited by Cherenkov radiation (see Fig. 7 in Ref. 3).

V. NUMERICAL MODELING

To get a better insight into experimental data, we performed numerical simulations of the coupled sine-Gordon equation with nonradiating boundary conditions (see Refs. 3 and 8 for details of the numerical procedure, analysis of Fiske steps with proper radiative boundary conditions can be found in Ref. 26). To reproduce the real situation, we introduced a small gradient of I_c (5% per IJJ) from the top to the bottom of the mesa. We also considered the presence of the bulk crystal below the mesa and the additional top deteriorated junction.[12] To model the crystal, we introduced an additional junction at the bottom of the stack with zero net bias current. The additional top junction was assumed to have a 100 times smaller I_c. Passive top and bottom junctions do not cause any principle differences in fluxon dynamics. Although they may participate in geometrical resonances, they do not contribute to the flux-flow voltage. In simulations we used parameters of the mesa 1: $N=8$, $L=3.5\lambda_J\simeq2.4$ μm, and the damping coefficient $\alpha=0.01-0.05$. Small damping is important for excitation of a large variety of geometrical resonances. In order to reach various resonances the bias current was swept back and forth several times, mimicking experimental measurement.

Figures 5(a) and 5(b) show simulated I-V curves (with subtracted top junction resistance) at $\Phi/\Phi_0=4.0$ for the case of uniform damping $\alpha_i=0.01$ $(i=1,2,\ldots,8)$. Panel (b) shows the total dc voltage in a wide current range (current is normalized by the total QP resistance of the mesa). Basically all geometrical resonances with velocities from c_8 to c_1 are seen, consistent with previous simulations.[16,17]

Panel (a) shows details of the subluminal flux-flow branch, $u_{FF}<c_8$. Here also a large variety of Fiske steps is seen. The most frequent step separation is $V_{1,8}$ and $2V_{1,8}$ (the grid spacing). The largest collective step occurs at $8V_{7,8}$ close to the velocity-matching condition, Eq. (9). However, a finer step structure with different voltages is developing in the top half of the flux-flow branch at $V>2.5$ mV. To understand its origin, in the inset we show individual voltages for all junctions. Vertical lines indicate positions of all possible Fiske steps $V_{m,n}$. The most prominent modes (m,n) are indicated. As expected, in the considered case of integer Φ/Φ_0 only odd $m=1,3,5,7$ resonances are excited. The observed even $2V_{1,8}$ step separation is due to sequential switching between nearest odd-m steps, as discussed in connection with Fig. 3(c). However, not all steps in the subluminal regime are due to out-of-phase $n=8$ resonances. Several superluminal resonances, $n=3,4,5,6$, are also excited.

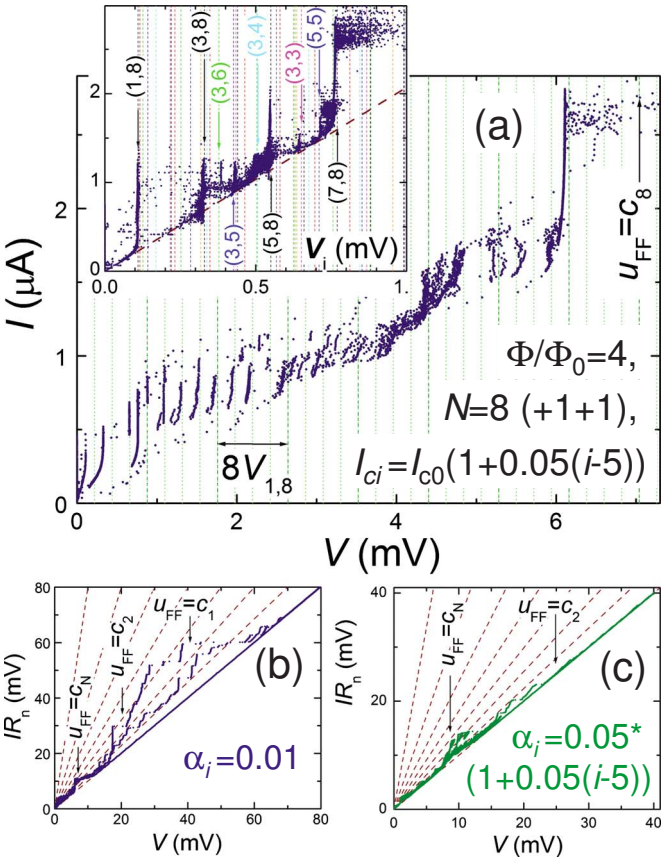

FIG. 5. (Color online) Simulated *I-V* characteristics at $\Phi/\Phi_0=4.0$ for a mesa with $N=8$ active IJJs and two passive junctions at the top and bottom of the mesa. Panels (a) and (b) represent simulations for a small nonuniformity of the critical current (5% per IJJ) and uniform damping parameter $\alpha_i=0.01$. (a) The subluminal $u_{\rm FF}<c_8$ part of the flux-flow characteristics. Inset shows *I-V* characteristics of individual junctions. Vertical lines show positions of all possible Fiske steps. Appearance of various superluminal resonances is indicated. (b) The *I-V* in a wider range. Dashed lines represent QP branches. Very strong superluminal Fiske steps are seen. Panel (c) shows the *I-V* characteristics of a mesa with nonuniform I_{ci} and $\alpha_i\simeq 0.05$, both increase by 5% per IJJ from the top to the bottom of the mesa. It is seen that variation in junction resistances strongly suppresses high-frequency resonances.

Our simulations demonstrate that superluminal resonances $c_n>c_N$ can be excited by subluminal flux flow $u_{\rm FF}<c_N$, which is in agreement with experimental data reported above. Although such possibility was not discussed before, it is probably not surprising because qualitatively the same happens with out-of-phase resonances. The necessary condition is given by Eq. (8), which clearly allows excitation of superluminal modes $n<N$ at $u_{\rm FF}<c_N$. For example, in the considered case $N=8$, the first fastest (1,1) mode can be excited at $u_{\rm FF}\simeq c_8$, provided $\Phi/\Phi_0>c_1/2c_8\simeq 3$.

A. Quality factors of different modes

The quality factor $Q=\omega RC$ is an important characteristic of the resonance. Here, R is the effective damping resistance and C the capacitance of the junction. High-quality geometrical resonances are crucial for realization of coherent FFOs:[26] (i) they amplify the emission power $P\propto E_{\rm ac}^2\propto Q^2$. This is especially important for stacked FFOs since there is no Lorentz contraction of the fluxon at the velocity-matching condition,[3] which is used for amplification of the electric field in a single junction FFO.[28] (ii) They reduce the radiation linewidth of the FFO $\propto 1/Q$. (iii) They may impose their order on the fluxon lattice even at subluminal flux-flow velocities, as follows from numerical simulations in Fig. 5(a). In particular, in-phase resonances may stabilize the rectangular fluxon lattice, facilitating coherent amplification of radiation $P\propto Q^2N^2$. The forced transformation of the fluxon lattice occurs when the resonant standing-wave electric field $E_{\rm ac}\propto 1/Q$ is larger than the fields of the fluxons. Therefore, high Q is critical for such forced transformation.

Although numerical simulations presented above describe well the subluminal $u_{\rm FF}<c_8$ part of experimental flux-flow branches [cf. Figs. 3 and 5(a)], there is a clear discrepancy in the superluminal regime. Numerical simulations[16,17] predict very strong superluminal Fiske steps, which have even larger amplitudes than the out-of-phase steps at $u_{\rm FF}\leq c_8$, as seen from Fig. 5(b). In those simulations larger Q for higher Fiske steps is simply the consequence of linear growth of $Q\propto\omega$ for constant R and C. To clarify this discrepancy we consider the quality factors of different modes (m,n),

$$Q_{m,n}=\frac{\pi c_n mR(\omega)C}{L}. \tag{10}$$

Here L is the junction length. There are two counteracting contributions. On the one hand, $Q\propto\omega_{m,n}$ and should be larger for high speed and large m modes. On the other hand, the effective resistance $R(\omega)$ is decreasing with increasing frequency. For single Josephson junctions it is very well established that at high frequencies $R(\omega)$ is approaching the radiative resistance of the circuitry $R_{\rm rad}\sim 50\ \Omega$ (Ref. 46) due to predominance of radiative losses into outer space.

As emphasized in Ref. 26, in stacked junctions $R(\omega)$ strongly depends on n. Out-of-phase modes interfere destructively, canceling radiative losses. Therefore, Q of those nonemitting modes is determined by the large QP resistance $R_{\rm QP}$,

$$Q_{m,N}=\frac{\pi c_N mR_{\rm QP}C}{L}. \tag{11}$$

Taking parameters for our mesa 1, $c_N\simeq 3.17\times 10^5$ m/s, $R_{\rm QP}\simeq 2$ kΩ at $T=1.6$ K, intrinsic capacitance $C\simeq 70$ fF/μm^2, $L=2.7$ μm, $L_y=1.4$ μm, and $m=2$ we obtain $Q_{2,8}\simeq 390$. This very large value is consistent with the sharp, large amplitude (2,8) steps seen in Fig. 3(a). It is also consistent with observation of out-of-phase Fiske steps in much longer junctions $L=50$ μm.[32] The same is true for other destructively interfering, nonradiative modes

$$n^*=N-2i,\quad i=0,1,2,\ldots,\text{int}[(N-1)/2]. \tag{12}$$

For the in-phase mode electric fields from all junctions interfere constructively resulting in large coherent emission. In this case R is determined by radiative losses,

$$Q_{m,1} = \frac{\pi c_1 m R_{\rm rad} C}{L}. \quad (13)$$

Using parameters of mesa 1, $c_1 \simeq 1.8 \times 10^6$ m/s, and assuming $R_{\rm rad}=50\ \Omega$ we obtain $Q_{2,1} \simeq 46$. Thus, radiative geometric resonances should have substantially smaller Q than the nonradiative ones.[26]

For mesa 1 with $N=8$ all even-n modes are nonradiative, Eq. (12). Fiske steps due to such resonances should have the highest Q and amplitude. This is consistent with our observation that even-n modes correspond to the most prominent Fiske steps, see Fig. 3. Similarly, more smeared, high-voltage Fiske steps at larger fields could indicate enhanced emission and radiative losses from the radiative superluminal resonances. The asymmetry between even and odd n Fiske steps is an indirect evidence for significant coherent radiation emission from the stack.[26]

B. Suppression of superluminal resonances by the spread in junction resistances

Collective, high-voltage Fiske steps can also be suppressed by another trivial reason; due to the spread in junction resistances ΔR. Indeed, if junctions in the stack have slightly different QP resistances R_i, the Fiske step $V_{m,n}$ would occur at different currents $I_i = V_{m,n}/R_i$. Therefore, the collective Fiske step could be observed only if the amplitude of the steps $\Delta I > (V_{m,n}/R_i^2)\Delta R$. Apparently, this condition is more difficult to satisfy for high voltage and low Q resonances.

To demonstrate this, in Fig. 5(c) we present numerical simulations for nonuniform damping $\alpha_i \simeq 0.05$, increasing by 5% per IJJ from the top to the bottom of the mesa and with the corresponding spread in the QP resistances $R_i \propto 1/\alpha_i$. The rest of the parameters are similar to that in panels (a) and (b). From comparison with panel (b) it is clear that the amplitude of low-frequency out-of-phase c_N steps $IR_n \simeq 10$ mV is unchanged but all high-frequency superluminal resonances are strongly reduced. The fastest in-phase resonances are practically nonexisting. We emphasize that in the considered case this is not due to radiative losses but is caused by the trivial reason that junctions cannot be synchronized because it is impossible to keep them at the same voltage for a given current. Note that the spread in I_c is not preventing the synchronization and is, therefore, much less detrimental for resonances, as seen from Fig. 5(b). In practice, both low Q due to radiative losses[26] and enhanced sensitivity to resistance spread may explain the abundance of the highest speed Fiske steps in experiment.

VI. CONCLUSIONS

In conclusion, careful alignment of magnetic field allowed observation of a large variety of Fiske steps in small Bi-2212 mesas. Small number of IJJs in the mesa allowed accurate identification of different resonant modes. Different resonance modes, including superluminal with velocities larger than the lowest velocity of electromagnetic waves c_N, were observed. It was shown both experimentally and theoretically that superluminal geometrical resonances can be excited in the subluminal flux-flow state. Superluminal flux-flow state with the maximum flux-flow velocity up to the Swihart velocity $c_0 \simeq 1.4 c_N$ was also reported. The most prominent observed Fiske steps correspond to nonemitting resonance modes n^*, Eq. (12). The corresponding asymmetry between even and odd-n resonances can be viewed as indirect evidence for significant coherent emission from intrinsic Josephson junctions.[26]

ACKNOWLEDGMENTS

We are grateful to A. Tkalecz for assistance with sample fabrication. The work was supported by the K. & A. Wallenberg foundation, the Swedish Research Council, and the SU-Core Facility in Nanotechnology.

*vladimir.krasnov@fysik.su.se

[1] D. W. McLaughlin and A. C. Scott, Phys. Rev. A **18**, 1652 (1978).
[2] A. Laub, T. Doderer, S. G. Lachenmann, R. P. Huebener, and V. A. Oboznov, Phys. Rev. Lett. **75**, 1372 (1995).
[3] V. M. Krasnov, Phys. Rev. B **63**, 064519 (2001). Note the reverse numeration of the modes there: $n=1$ is the slowest and $n=N$ is the fastest mode.
[4] S. Sakai, A. V. Ustinov, H. Kohlstedt, A. Petraglia, and N. F. Pedersen, Phys. Rev. B **50**, 12905 (1994).
[5] S. Sakai, A. V. Ustinov, N. Thyssen, and H. Kohlstedt, Phys. Rev. B **58**, 5777 (1998).
[6] R. Kleiner, Phys. Rev. B **50**, 6919 (1994).
[7] G. Hechtfischer, R. Kleiner, A. V. Ustinov, and P. Müller, Phys. Rev. Lett. **79**, 1365 (1997).
[8] V. M. Krasnov and D. Winkler, Phys. Rev. B **56**, 9106 (1997).
[9] S. Savel'ev, V. A. Yampol'skii, A. V. Rakhmanov, and F. Nori, Rep. Prog. Phys. **73**, 026501 (2010).
[10] P. Barbara, A. B. Cawthorne, S. V. Shitov, and C. J. Lobb, Phys. Rev. Lett. **82**, 1963 (1999).
[11] S. V. Shitov, A. V. Ustinov, N. Iosad, and H. Kohlstedt, J. Appl. Phys. **80**, 7134 (1996).
[12] V. M. Krasnov, Phys. Rev. B **79**, 214510 (2009).
[13] I. E. Batov, X. Y. Jin, S. V. Shitov, Y. Koval, P. Müller, and A. V. Ustinov, Appl. Phys. Lett. **88**, 262504 (2006).
[14] L. Ozyuzer, A. E. Koshelev, C. Kurter, N. Gopalsami, Q. Li, M. Tachiki, K. Kadowaki, T. Yamamoto, H. Minami, H. Yamaguchi, T. Tachiki, K. E. Gray, W. K. Kwok, and U. Welp, Science **318**, 1291 (2007).
[15] M. H. Bae, H. J. Lee, and J. H. Choi, Phys. Rev. Lett. **98**, 027002 (2007).
[16] R. Kleiner, T. Gaber, and G. Hechtfischer, Physica C **362**, 29 (2001).
[17] M. Machida, T. Koyama, A. Tanaka, and M. Tachiki, Physica C **330**, 85 (2000).
[18] A. E. Koshelev and I. S. Aranson, Phys. Rev. Lett. **85**, 3938

(2000).
[19] D. A. Ryndyk, V. I. Pozdnjakova, I. A. Shereshevskii, and N. K. Vdovicheva, Phys. Rev. B **64**, 052508 (2001).
[20] V. M. Krasnov, Phys. Rev. Lett. **103**, 227002 (2009); **97**, 257003 (2006).
[21] L. N. Bulaevskii and A. E. Koshelev, Phys. Rev. Lett. **99**, 057002 (2007).
[22] X. Hu and S. Z. Lin, Supercond. Sci. Technol. **23**, 053001 (2010).
[23] T. Tachiki and T. Uchida, J. Appl. Phys. **107**, 103920 (2010).
[24] M. Tachiki, S. Fukuya, and T. Koyama, Phys. Rev. Lett. **102**, 127002 (2009).
[25] K. Kadowaki, M. Tsujimoto, K. Yamaki, T. Yamamoto, T. Kashiwagi, H. Minami, M. Tachiki, and R. A. Klemm, J. Phys. Soc. Jpn. **79**, 023703 (2010).
[26] V. M. Krasnov, arXiv:1005.2963 (unpublished).
[27] H. B. Wang, S. Guenon, B. Gross, J. Yuan, Z. G. Jiang, Y. Y. Zhong, M. Gruenzweig, A. Iishi, P. H. Wu, T. Hatano, D. Koelle, and R. Kleiner, arXiv:1005.0081 (unpublished).
[28] V. P. Koshelets and S. V. Shitov, Supercond. Sci. Technol. **13**, R53 (2000).
[29] S. O. Katterwe and V. M. Krasnov, Phys. Rev. B **80**, 020502(R) (2009).
[30] V. M. Krasnov, V. A. Oboznov, V. V. Ryazanov, N. Mros, A. Yurgens, and D. Winkler, Phys. Rev. B **61**, 766 (2000).
[31] V. M. Krasnov and D. Winkler, Phys. Rev. B **60**, 13179 (1999); V. M. Krasnov, *ibid.* **60**, 9313 (1999).
[32] V. M. Krasnov, N. Mros, A. Yurgens, and D. Winkler, Phys. Rev. B **59**, 8463 (1999).
[33] S. M. Kim, H. B. Wang, T. Hatano, S. Urayama, S. Kawakami, M. Nagao, Y. Takano, T. Yamashita, and K. Lee, Phys. Rev. B **72**, 140504(R) (2005).
[34] Y. I. Latyshev, A. E. Koshelev, V. N. Pavlenko, M. B. Gaifullin, T. Yamashita, and Y. Matsuda, Physica C **367**, 365 (2002).
[35] Y. D. Jin, H. J. Lee, A. E. Koshelev, G. H. Lee, and M. H. Bae, EPL **88**, 27007 (2009).
[36] M. H. Bae, J. H. Choi, and H. J. Lee, Phys. Rev. B **75**, 214502 (2007).
[37] S. J. Kim, T. Hatano, and M. Blamire, J. Appl. Phys. **103**, 07C716 (2008).
[38] A. L. Fetter and M. J. Stephen, Phys. Rev. **168**, 475 (1968).
[39] I. O. Kulik, JETP Lett. **2**, 84 (1965).
[40] I. M. Dmitrenko, I. K. Yanson, and V. M. Svistunov, JETP Lett. **2**, 10 (1965); M. Cirillo, N. Gronbech-Jensen, M. R. Samuelsen, M. Salerno, and G. V. Rinati, Phys. Rev. B **58**, 12377 (1998).
[41] V. M. Krasnov, Phys. Rev. B **65**, 140504 (2002).
[42] V. M. Krasnov, T. Bauch, and P. Delsing, Phys. Rev. B **72**, 012512 (2005).
[43] A. Irie, S. Kaneko, and G. I. Oya, Int. J. Mod. Phys. B **13**, 3678 (1999).
[44] See supplementary material at http://link.aps.org/supplemental/10.1103/PhysRevB.82.024517 for magnetic field modulation of Fiske steps and the critical current, which can be seen in the accompanying animation.
[45] H. B. Wang, S. Urayama, S. M. Kim, S. Arisawa, T. Hatano, and B. Y. Zhu, Appl. Phys. Lett. **89**, 252506 (2006).
[46] J. M. Martinis, M. H. Devoret, and J. Clarke, Phys. Rev. B **35**, 4682 (1987).